A Semi-automated Image Segmentation Approach for Computational Fluid Dynamics Studies of Aortic Dissection

Jeff R. Anderson, Christof Karmonik, Yannick Georg, Jean Bismuth, Alan B. Lumsden, Adeline Schwein, Mickael Ohana, Fabien Thaveau, and Nabil Chakfé

Abstract— **Computational studies of aortic hemodynamics require accurate and reproducible segmentation of the aortic tree from whole body, contrast enhanced CT images. Three methods were vetted for segmentation. A semi-automated approach that utilizes denoising, the extended maxima transform, and a minimal amount of manual segmentation was adopted.**

I. Introduction

Hemodynamics in the ascending and descending aorta can be altered by patient-specific geometries and inflow rates [1]. In order to further understand the hemodynamics incident to aortic dissection, as well as the effects of stent graft placement upon these hemodynamics, computational fluid dynamics studies have recently been carried out on 3D virtual models of clinical cases acquired from high resolution CT scans [2,3]. Accurate and timely segmentation of the main arterial tree is required to facilitate such studies.

Threshold-based methods of image segmentation are challenged by intensity gradients within the image volume. Edge detection methods are challenged by poor contrast in the image. CT scans of aortic dissections may suffer from both. Due to velocity gradients resulting from dissection, intensity gradients often exist along the longitudinal axis of the aortic tree. Furthermore, dissimilar gradients may exist in the different layers of the dissection.

Figure 1 illustrates this issue. The figure shows two images taken from a single CT scan of an aortic tree with a dissection. The two images are windowed identically, however, there is much greater contrast between the two layers of the dissection in one of the two images. In addition, the signal intensity level observed in the aorta is not consistent in the two images. This is particularly noticeable in the layer of the dissection that appears on the right of panel B. This layer corresponds to the smaller layer seen on the bottom of panel A.

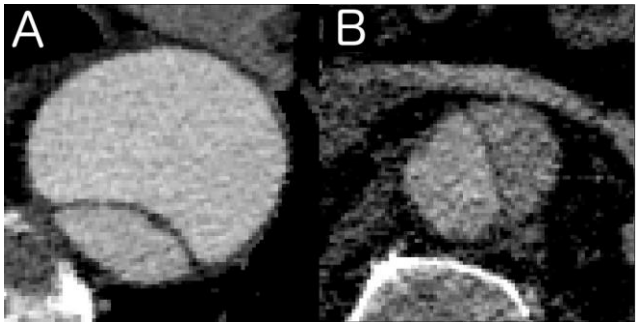

Figure 1. Two images from a single descending aorta with a dissection; windowing is identical in both images. One slice slice is located just distal the aortic arch (A). The other is located just proximal the aortic bifurcation (B).

In this paper, a semi-automated methodology is set forth for segmentation of the aortic tree for computational fluid dynamics studies of aortic dissection. The method increases the reliability of segmentation as compared to threshold-based methods. It also increases throughput of segmentation as compared to a manual approach.

II. Methods

A. CT Image Acquisition

All CT Images were acquired on a Toshiba whole body CT scanner following contrast administration with FOV = 512 x 512 x 857 and

J. R. Anderson and C. Karmonik are with the MR Core Facilities at the Houston Methodist Research Institute, Houston, TX 77030 USA (phone: 713-441-0803; fax: 771-441-0845; e-mail: JRAnderson@houstonmethodist.org and CKarmonik@houstonmethodist.org).

J. Bismuth and A. B. Lumsden are with the Houston Methodist DeBakey Heart & Vascular Center at Houston Methodist, Houston, TX 77030 USA (email: ABLumsden@houstonmethodist.org and JBismuth@houstonmethodist.org)

N. Chakfé, Y. Georg, A. Schwein, and F. Thaveau are with the University Hospital of Strasbourg, Strasbourg, Department of Vascular Surgery and Kidney Transplantation, 67085 France (email: nabil.chakfe@chru-strasbourg.fr, yannick.georg@chru-strasbourg.fr, adeline.schwein@chru-strasbourg.fr, and Fabien.thaveau@chru-strasbourg.fr).

M. Ohana is with the University Hospital of Strasbourg, Strasbourg, Department of Diagnostic Radiology, 67085 France (email:mickael.ohana@chru-strasbourg.fr)

978-1-4244-7929-0/14/$26.00 ©2014 IEEE

res = 0.866 x 0.866 x 0.801. In total, 27 datasets were acquired.

B. Threshold-based Segmentation Approach

CT images were first cropped roughly in imagej to include the region immediately surrounding the aortic tree [4]. The cropped images were then windowed to highlight the aortic tree. These initial steps were carried out for all three segmentation approaches; a resultant image is illustrated in Figure 2. The image volume was then visualized in Paraview [5]. A thresholded contour was applied to the volume. The threshold level was manually optimized in order to segment the aortic tree from the surrounding tissue. A connectivity filter was applied to the resultant isosurface and the estimation of the aortic tree was extracted.

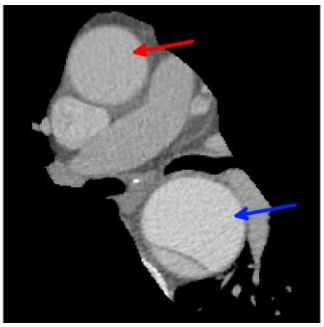

Figure 2. A single image from the CT dataset after a rough cropping and windowing. The ascending aorta is indicated with a red arrow and the descending aorta is indicated with a blue arrow.

C. Edge Detection Segmentation Approach

The cropped and windowed dataset was loaded into Matlab [6]. Next, the Sobel method was used for edge detection on a slice-by-slice basis (Matlab Image Processing Toolbox). The resultant edges were dilated with a disk-shaped structuring element. A seed point was marked on the interior of the aorta in a single slice located near the aortic bifurcation in order to locate a region of interest outlined by the dilated edge. The centroid of the selected region of interest was passed as the seed point to the neighboring slice(s) and the process was iterated for all slices. The process was repeated with the initial seed point located in the ascending aorta and the two resultant data masks manually combined. The mask was applied to the data and introduced into Paraview for comparison with other methods.

D. Semi-automated Segmentation Approach

The cropped and windowed dataset was loaded into Matlab. Next, the image was denoised with the total noise variation method [7]. The resultant images were segmented using an extended maxima transform (i.e., the imextendedmax Matlab function) [8]. The images were then manually edited to separate the aortic tree from tissue falsely identified as belonging to the aorta. An aortic mask was then retrieved following the same method of centroid seeding described in section C. The mask was applied to the data and introduced into Paraview for comparison with other methods.

III. RESULTS

The threshold approach was found to correctly segment the upper portion of the descending aorta, but underestimated the ascending aorta and the lower portion of the descending aorta. The edge detection approach was found to correctly segment the ascending aorta and the upper portion of the descending aorta, but underestimated the lower portion of the descending aorta. The semi-automated approach was found to correctly segment all portions of the aortic tree.

Representative slices from each of the three approaches are shown in Figure 3. The two slices shown for each method, respectively, are matched and are physically located close to those shown in Figure 1.

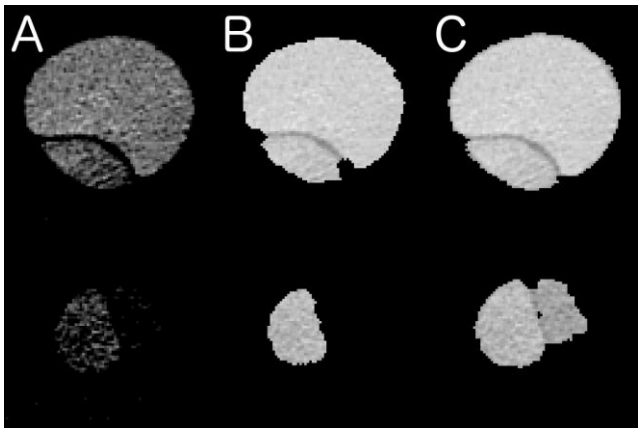

Figure 3. Representative segmentation results for the threshold approach (A), the edge detection approach (B), and the semi-automated approach (C). In each panel, the slice displayed on top is located just distal the aortic arch and the slice displayed on bottom is located just proximal the aortic bifurcation.

IV. DISCUSSION

Figure 3 demonstrates that the threshold approach (Panel A) is not able to compensate for the gradation in signal intensity along the

longitudinal axis of the aorta. The result is a fairly correct segmentation in the top slice, but poor segmentation in the bottom slice. Due to the lower S/N in the bottom slice, one of the two layers is lost and the other is poorly segmented.

The edge detection approach (Figure 3, Panel B) outperforms the threshold approach. One of the two layers of the aorta is preserved in the bottom slice without error. However, the other layer is still lost. Presumably, this is due to the lack of contrast between the second, lost layer and the surrounding tissue. That is, the contrast between the two layers was greater than the contrast between the lower intensity layer and the surrounding tissue.

The semi-automated approach (Figure 3, Panel C) segments both of the representative slices without loss of either layer. This approach, however, does include some manual segmentation. Figure 4 demonstrates a representative segmentation step. Manual segmentation of this nature was required for 20-25% of slices. However, as is illustrated in Figure 4, the segmentation steps were minor. They most often consisted of a single "stroke" per slice resulting in rapid and reliable segmentation.

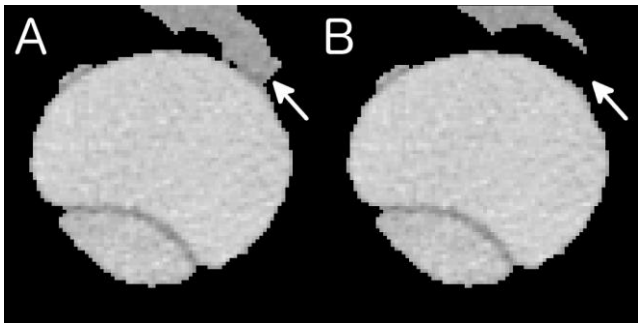

Figure 4. This figure illustrates the manual segmentation required for a single slice in the semi-automated approach. The slice before manual segmentation is shown on the left (A). The slice after manual segmentation is shown on the right (B). The arrow highlights the small portion of tissue that was seperated from the aorta.

Isosurfaces obtained using the semi-automated method are shown in Figure 5 for three representative aortic trees. 3D printing of isosurface models was used to visually evaluate the final segmented surface (Figure 6).

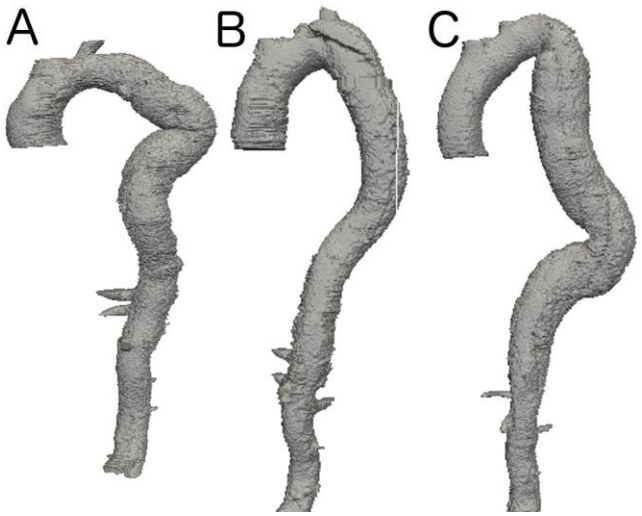

Figure 5. Isosurfaces from three representative aortic trees.

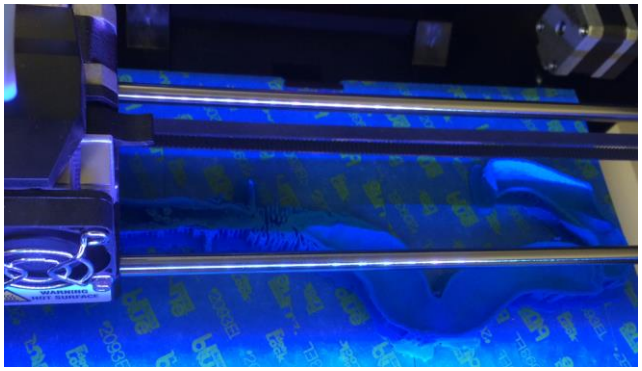

Figure 6. Aortic trees were 3D printed.

V. Conclusion

In conclusion, the semi-automated approach consisting of denoising, segmentation via the extended maxima transform, and limited manual segmentation was found to most accurately segment the aortic tree. This method has been adopted to support ongoing computational fluid dynamics studies. Comparison of the method with other reported methods [9] presents an additional interesting future direction for this work.

References

[1] C. Karmonik, J. X. Bismuth, M. G. Davies, and A. B. Lumsden, "Computational hemodynamics in the human aorta: A computational fluid dynamics study of three cases with patient-specific geometries and inflow rates," *Technology and Health Care*, vol. 16, pp. 343–354, June 2008.

[2] C. Karmonik, J. Bismuth, M. G. Davies, D. J. Shah, H. K. Younes, and A. B. Lumsden, "A Computational Fluid Dynamics Study Pre- and Post-Stent Graft Placement in an Acute Type B Aortic Dissection," *Vascular and Endovascular Surgery*, Vol. 45(2), pp. 157-164, Mar. 2011.

[3] C. Karmonik, J. Bismuth, D. J. Shah, M. G. Davies, D. Purdy, and A. B. Lumsden, "Computational Study of Haemodynamic Effects of Entry- and Exit-Tear Coverage in a DeBakey Type III Aortic Dissection: Technical Report," *European Journal of Vascular and Endovascular Surgery*, vol. 42(2), pp. 172-177, Aug. 2011.
[4] W. S. Rasband, ImageJ. [Online]. Available: https://imagej.nih.gov
[5] A. Henderson, Paraview. [Online]. Available: https://www.paraview.org
[6] MATLAB version 8.2.0. Natick, Massachusetts: The Mathworks, Inc. 2013.
[7] P. Getreuer, "Rudin-Osher-Fatemi Total Variation Denoising using Split Bregman," *Image Processing On Line*, 2012.
[8] P. Soille, *Morphological Image Analysis: Principles and Applications*. Springer-Verlag, 1999, pp.170-171.
[9] S. Kurugol, R. S. J. Estepar, J. Ross, G. R. Washko, "Aorta Segmentation with a 3D Level Set Approach and Quantification of Aortic Calcifications in Non-contrast Chest CT," *Conf Proc IEEE Eng Med Biol Soc*, pp. 2343-2346, 2012.